

## **ANALYSIS OF SEISMIC BEHAVIOR OF DOUBLE BACK-TO-BACK C STEEL FRAME WITH GUSSET PLATE**

Ming Chen<sup>1</sup>, Fangfang Sun<sup>2,a</sup> and Mengqi Li<sup>1</sup>

<sup>1</sup>Architecture and Civil Engineering School, Inner Mongolia University of Science and Technology, Baotou 014010, P.R. China

<sup>2</sup>Civil and Architecture Engineering School, ZhengZhou University of Science and Technology, Zhengzhou 450007, P.R. China

<sup>a</sup>[Corresponding Author, E-mail: 819447764@qq.com](mailto:819447764@qq.com)

### **ABSTRACT**

In this paper, the frame structure of double cold-formed thin-walled C steel back to back connected with gusset plate was studied. The seismic behavior of three single-story and single-span frames was studied through both pseudo-static tests and finite element analysis. The hysteretic curves, skeleton curves and strain distribution were obtained by low cyclic loading. Two influencing factors, i.e. axial compression ratio and pitch of bolts, were also fully considered; the failure mechanism, bearing capacity, rigidity degradation, ductility and energy dissipation of the frames were carefully studied. The results revealed that all of the failure patterns of the frames indicated instability in load plane and local buckling at beam end and column base web. The axial compression ratio had greater impact on bearing capacity and rigidity degradation than the factor of bolt pitch. The ductility coefficient and energy dissipation of this structure accorded with the design requirements.

**KEYWORDS:** C Steel Frame, Seismic Behavior Study, Axial Compression Ratio, Pitch of Bolts

### **INTRODUCTION**

Cold-formed thin-walled steel structure, which is characterized by its light weight, environmental protection, energy saving and high efficiency, and superiority to the traditional hot-rolled H-steel structure, has been used widely in architectural markets as the main bearing structure in the construction of long-span buildings with no tower crane used. In China, especially after the 2008 Wenchuan Earthquake, a growing emphasis has been put on seismic behavior of the structures (Zhou et al., 2008), which makes the cold-formed thin-walled steel structure increasingly popular with residents and constructors. Over the past eight years, extensive tests and analytical researches on the seismic behavior of bending joints have been conducted in Inner Mongolia University of Science and Technology of the cold-formed C steel back to back connected with gusset plate. The plate thickness, C steel type, pitch and diameter of bolts have been well considered, and the influence of these factors to the bending capacity of the joints has been extensively investigated. Meanwhile, an effective analytical model was founded to analyze this kind of structure.

Comparison of the related research works (DeWolf et al., 1974; Schafer, 2002; Liu et al., 2009a; Liu et al., 2009b; Shen et al., 2013) showed that currently there are many studies reported on cold-formed steel structure, which are mostly applied in the joints and walls. There are, however, few studies on the framework. This study took double C steel framework as its object. The seismic behavior of the frame with this cross-sectional form has been studied through both tests and finite element analyses. The two influencing parameters, i.e. axial compression ratio of column and pitch of bolts of beam-column joint, were considered in the seismic behavior of the overall framework. The process of damage, bearing capacity and rigidity degradation, energy dissipation capacity and ductility of the framework were respectively analyzed. With the gusset plate, the node rigidity was enhanced, making the seismic behavior of the overall framework superior to that of other cold-formed structural systems.

### **DESIGN OF THE FRAMES**

Three single-story and single-span frames with this cross-sectional form were selected to study their seismic behavior by low cyclic load tests (Huang, 2010) and ANSYS10.0 finite element analysis (Shi et al., 2011). The span of the framework was 1600mm and the height was 960mm, the gusset plate of beam-column joint was pentagon and the stiffener plate of column base was isosceles trapezoid, the column

base had a 20mm thick rectangular hot rolled steel plate. 8.8 M20 high-bearing capacity bolts with friction type (Zhang and Du, 1999; Wang, 2006) were used with pre-tension as 125 kN. The framework parameters are shown in Table 1, the test equipment and finite element model are shown in Fig. 1 and Fig. 2, respectively.

**Table 1: Frame Parameters**

Frame numbers	Beam section(mm)	Column section(mm)	Gusset plate thickness(mm)	Pitch of bolts (mm)	Axial pressure (kN)
KJ1	C120×50×20×2	C160×50×20×2	8	120	40
KJ2	C120×50×20×2	C160×50×20×2	8	60	40
KJ3	C120×50×20×2	C160×50×20×2	8	60	0

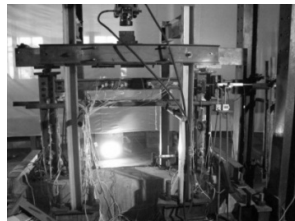


Fig. 1 Test equipment

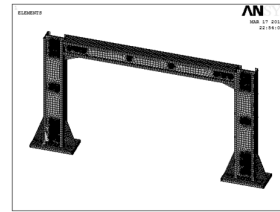


Fig. 2 Finite element model

The material tests on raw materials were conducted to get the behavior of the steel which could be used for test and finite element analysis. The test results of cold-formed thin-walled C steel are shown in Table 2.

**Table 2: Material Behavior Results**

Steel Model	Yield bearing capacity (N/mm <sup>2</sup> )	Ultimate bearing capacity (N/mm <sup>2</sup> )	Elastic modulus (MPa)	Poisson's ratio	Elongation (%)
C160×50×20×2	265	389	1.96×10 <sup>5</sup>	0.26	26.9
C120×50×20×2	241	390	1.99×10 <sup>5</sup>	0.23	27.7

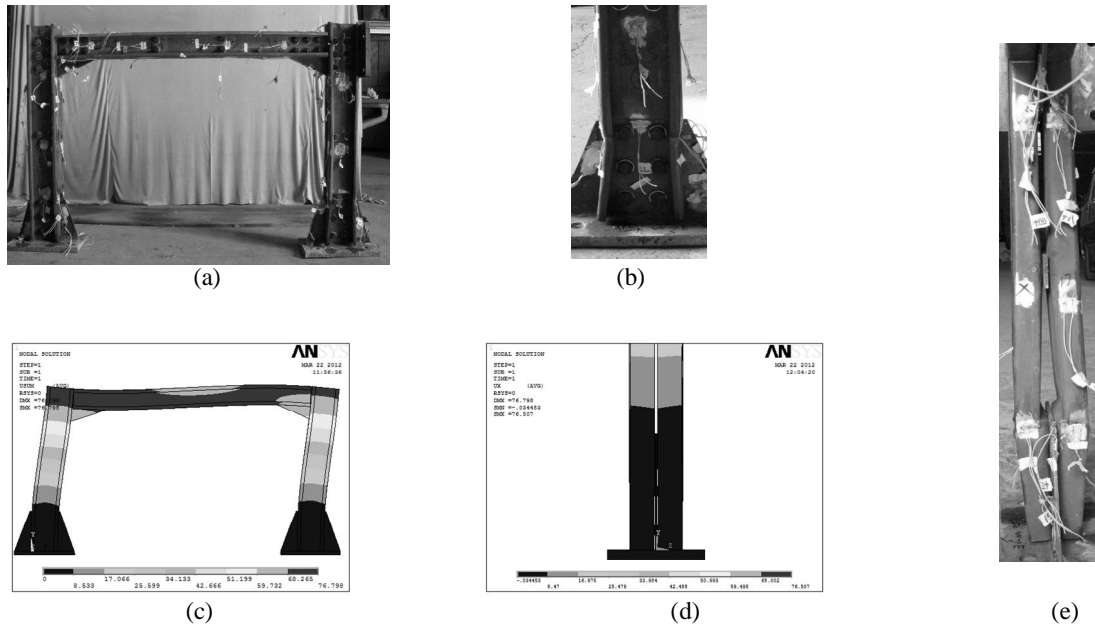
In this study, the mixed loading methods with load and displacement controlled were used in tests and finite element analysis, which were step loading with three times cycling. One loading grade (n) was taken as 3kN and 0.2Δy' after yielded, respectively. Δy' was the component deformation under the theoretical yield load.

## ANALYSIS OF TEST AND FINITE ELEMENT RESULTS

### 1. Framework Failure Patterns

All of the final failure patterns of the three frameworks were the overall flexural buckling; the control sections of the beam and column had large deformation, and the flanges on both sides of C steel of control sections of column base and beam-end were out-stretching, even with occurrence of rupture. Also, web buckling occurred at the same position and the flange edge was depressed to the web. Meanwhile, a similar study was conducted in Xi'an University of Architecture & Technology of China. The difference was that C steels were connected with self-drilling screws, and the framework had wall panels (Huang et al., 2011). It was reported that in the final failure pattern, the connections between wall panel and C steel were failed, and local buckling occurred in the wall studs. The two failure pattern results were a little different. In this study, only the KJ3 beam-end web had local buckling and the flange ruptured, having the

same results with the finite element analysis. These results reflect the influence of axial compression ratio on the failure patterns of the framework. The analytical failure pattern of KJ2 was similar to the test, as shown in Fig. 3.



(a) The test failure pattern (b) Test local buckling of column base  
 (c) The analytical failure pattern (d) Analytical local buckling of column base (e) Column failure pattern

Fig. 3 KJ2 Overall Instability and Local Buckling Shape

## 2. Hysteretic Curves

As it can be observed, the frame hysteretic curves shown in Fig. 4 were the typical fusiform. The shapes of hysteretic loop were complete and the elasto-plasticity had a large displacement. These phenomena reflected the better plastic deformation ability of the framework and the better seismic behavior of the structure.

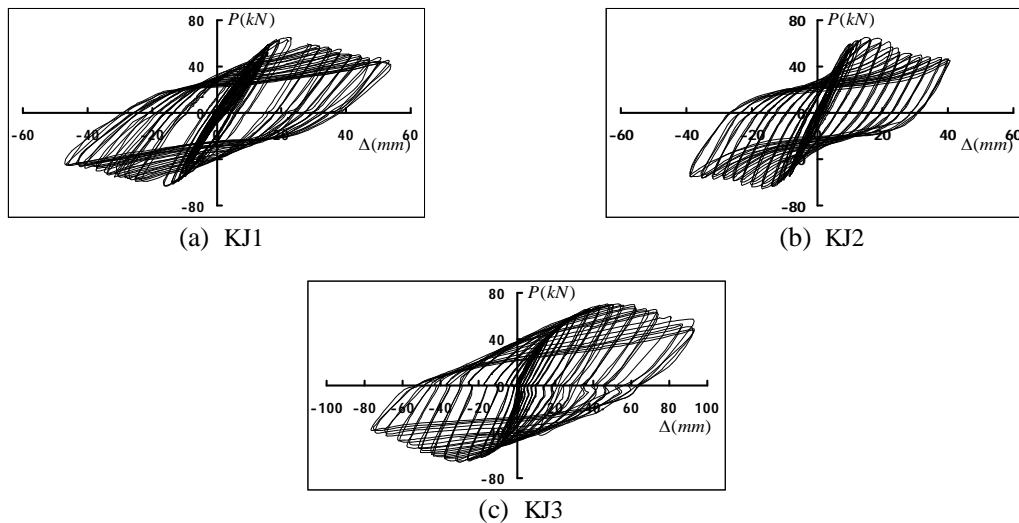


Fig. 4 Hysteretic Curves of Frames

### 3. Skeleton Curves

Comparison of the test results with the FE results of the maximum load and the corresponding displacement are shown in Table 3. The maximum load value was very close, the deviation was less than 5%. But the deviation of displacement values were wide variation (18%~39%), it revealed the nuance between the actual constitutive relation curves of frame steel and the elastic-plastic constitutive relation curves of the simulation during the plastic stage. Generally speaking, the FE results were consistent with the test results, proving that the model was practical and reliable.

**Table 3: Test and FE results**

Frame numbers	Maximum load (kN)		Maximum load to displacement(mm)		Load ratio	Displacement ratio
	Test values	FE values	Test values	FE values		
KJ1	63.26	65.31	23.62	16.10	1.032	0.682
KJ2	65.53	66.29	19.72	12.05	1.012	0.611
KJ3	70.45	71.67	53.54	44.07	1.017	0.823

According to the results of the analysis, the skeleton curves of the three frames were drawn, as shown in Fig. 5. Through comparison of the skeleton curves of KJ2 and KJ3, it was observed that the bearing capacity of the frame increased with the decrease of axial compression ratio. The bearing capacity increased by 7.51% when the axial pressure decreased from 40 kN to 0 kN. Comparison of the skeleton curves of KJ1 and KJ2 showed that the frame bearing capacity increased with decrease in the pitch of bolts. The bearing capacity increased by 3.59% when the pitch of bolts is decreased from 120 mm to 60 mm.

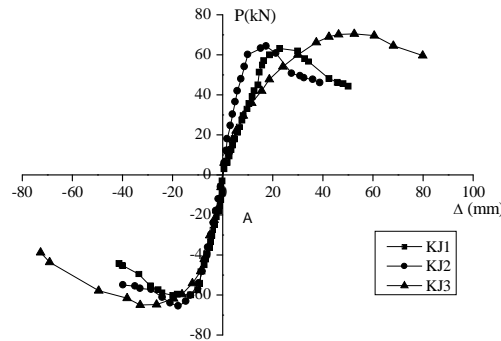


Fig. 5 Skeleton Curves of Frames

## ANALYSIS OF THE SEISMIC BEHAVIOR

### 1. Bearing Capacity Degradation

The bearing capacity degradation is the reduction in the bearing capacity of the structural members with the increase of the number of repeated loading under constant displacement conditions. The coefficient of bearing capacity degradation is defined as follows:

$$\lambda_i = \frac{F_j^i}{F_j^{i-1}} \quad (1)$$

in which  $\lambda_i$  is the  $i^{th}$  coefficient of bearing capacity degradation,  $F_j^i$  is the  $i^{th}$  load cycle peak point load value at the  $j^{th}$  displacement loading,  $F_j^{i-1}$  is the  $i-1^{th}$  load cycle peak point load values at the  $j^{th}$  displacement loading.

The bearing capacity degradation coefficients of the frame under the different grades of load bearing are shown in Fig. 6, in which  $\lambda$  is the coefficient of bearing capacity degradation,  $n$  is the loading grade. Bearing capacity degradation coefficients were greater than 0.9, and the value of each cycle was stable, the influence of cycling times on bearing capacity of the framework was smaller.

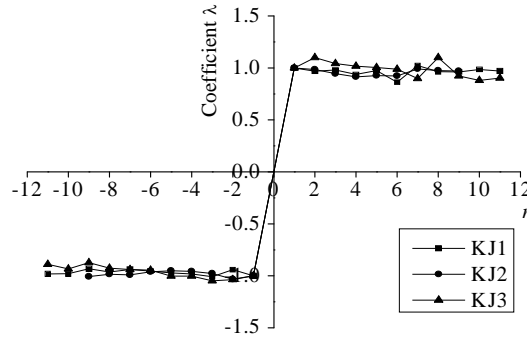


Fig.6 Bearing Capacity Degradation Coefficient of Frames

## 2. Rigidity Degradation

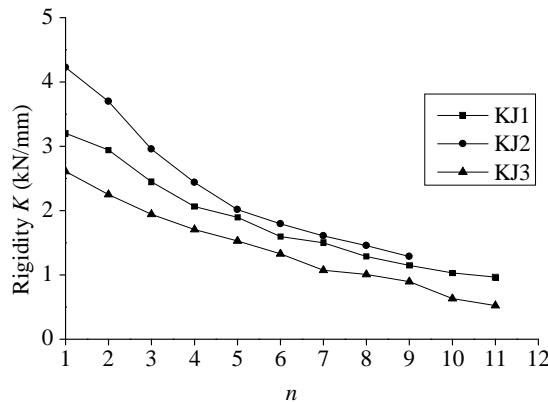


Fig.7 Rigidity Degradation of Frames

Rigidity degradation is defined as the reduction in rigidity of the structure with the increase in the repeated loading cycles under constant displacement conditions. The secant rigidity method was adopted to study the framework structure rigidity degradation, and the formula is shown as follows:

$$K_i = \frac{|+F_i| + |-F_i|}{|+X_i| + |-X_i|} \tag{2}$$

in which  $K_i$  is the  $i^{th}$  rigidity of the framework,  $F_i$  is the  $i^{th}$  peak load value,  $X_i$  is the  $i^{th}$  peak displacement value.

The different rigidity values of framework which were calculated under different load grades shown in Fig. 7, in which  $K$  is the rigidity of the frame,  $n$  is the loading grade. The rigidity of the frames was between 2 and 5 at the first loading grade, and between 0.5 and 2 at the last loading grade. The rigidity of the three frameworks showed a linear degradation. From the results, it is known that the changing of axial compression ratio has obvious impact on the rigidity of the framework. The initial rigidity, namely, the rigidity under the first loading grade, increased nearly 62.05% with the increase of axial compression ratio, and the speed of rigidity degradation became slow. When the pitch of bolts changed from 120 mm

to 60 mm, the initial rigidity of component increased by 32.02%, and the speed of rigidity degradation did not change significantly. It can be seen that the rigidity degradation curve of KJ3 was the smoothest one, and the rigidity degradation was the least. There was a positive correlation between axial compression ratio and the lateral rigidity of the framework.

### 3. Energy Dissipation

**Table 4: Energy Dissipation Index of Frames**

Frame numbers		KJ1		KJ2		KJ3	
Loading grade ( $n$ )		$E$	$h_e$	$E$	$h_e$	$E$	$h_e$
Test results	1	1.19	0.19	1.12	0.18	0.98	0.16
	2	1.33	0.21	1.18	0.19	1.26	0.20
	3	1.54	0.25	1.39	0.22	1.44	0.23
	4	1.65	0.26	1.48	0.24	1.72	0.27
	5	1.67	0.27	1.51	0.24	1.86	0.30
	6	1.62	0.26	1.47	0.23	1.86	0.30
	7	1.62	0.26	1.52	0.24	1.97	0.31
	8	1.69	0.27	1.48	0.24	2.00	0.32
	9	1.71	0.27	1.56	0.25	1.82	0.29
	10	1.71	0.27	—	—	1.77	0.28
	11	1.70	0.27	—	—	1.75	0.28
FE results	1	1.32	0.21	1.24	0.20	1.09	0.17
	2	1.48	0.24	1.30	0.21	1.40	0.22
	3	1.71	0.27	1.54	0.25	1.61	0.26
	4	1.83	0.29	1.64	0.26	1.92	0.31
	5	1.85	0.29	1.67	0.27	2.07	0.33
	6	1.80	0.29	1.62	0.26	2.07	0.33
	7	1.80	0.29	1.68	0.27	2.20	0.35
	8	1.88	0.30	1.64	0.26	2.23	0.36
	9	1.90	0.30	1.72	0.27	2.03	0.32
	10	1.89	0.30	—	—	1.97	0.31
	11	1.88	0.30	—	—	1.90	0.30

Energy-consumption means that structures, under cyclic loading, absorb energy while loading and release energy while unloading. Then the difference between absorbing and releasing energy is consumed by the frame structure. The capacity of energy dissipation was measured by the energy dissipation coefficient ( $E$ ) and equivalent viscous damping coefficient ( $h_e$ ), which were calculated by the method of calculating the envelope area. Both the test results and FE results are shown in Table 4. It can be seen that the FE values were a bit higher than test values. The different results revealed that there were uncertain factors during the tests. The  $h_e$  of this framework gradually increased with the increasing of loading grade. The  $h_e$  of steel reinforced concrete structure and portal frame were around 0.3 and 0.5, respectively. The  $h_e$  of this framework were between 0.16 and 0.36, and lower than that of the other structure. What's more, the values were also lower than the value i.e. 0.64 to 1.12 of Xi'an University of Architecture & Technology's study (Huang, 2010), but accorded with the design requirements. When the pitch of bolts changed from 60 mm to 120 mm, the  $h_e$  increased by 12.61% and  $E$  increased by 14.00%. Moreover, the  $h_e$  increases by 19.74% and  $E$  increases by 21.33% with the axial pressure load decreasing from 40 kN to 0 kN.

#### 4. Ductility

Ductility, the ability of the structure and components to support plastic deformation when the bearing capacity does not reduce remarkably, is an important index to measure and assess the seismic behavior of a structure. It is expressed by ductility coefficient ( $\mu$ ) and calculated as follows:

$$\mu = \Delta_u / \Delta_y \tag{3}$$

in which  $\mu$  is the framework ductility coefficient;  $\Delta_u$  is the component deformation when the bearing capacity dropped to 85% of the ultimate bearing capacity;  $\Delta_y$  is the component deformation under the yield load.

The  $\mu$  of the frameworks are calculated in Table 5. It can be seen that the FE values were a bit higher than test values, but the values were close. It showed the  $\mu$  ranged between 1.65 and 2.82, and it was slightly higher than the value of normal concrete structures and portal frame, i.e. 1.10 to 2.00, but it was lower than the value in Xi'an University of Architecture & Technology's study, i.e. 2.49 to 5.32 (Huang, 2010). The  $\mu$  increased by 54.55% with the pitch of bolts increasing from 60mm to 120mm. When the axis pressure load decreased from 40 kN to 0 kN, the  $\mu$  increased by 21.33%.

**Table 5: Ductility Index of Frames**

Frame numbers			$P_y$ (kN)	$\Delta_y$ (mm)	$P_u$ (kN)	$\Delta_u$ (mm)	$\mu$
Test results	KJ1	push	39.28	12.78	56.63	32.57	2.55
		pull	36.31	12.53	49.56	35.32	2.82
	KJ2	push	36.44	25.26	55.03	41.76	1.65
		pull	36.16	14.88	50.71	25.54	1.72
	KJ3	push	42.10	30.09	59.62	57.85	1.92
		pull	42.00	25.00	57.84	48.55	1.94
FE results	KJ1	push	40.35	12.10	55.51	31.77	2.63
		pull	38.61	11.99	50.10	33.29	2.78
	KJ2	push	38.98	22.13	56.35	40.98	1.85
		pull	39.10	13.16	55.89	24.10	1.83
	KJ3	push	43.22	25.68	60.92	56.99	2.22
		pull	43.17	23.10	58.90	47.21	2.04

#### CONCLUSIONS

Based on the tests and finite element program for analyzing the failure patterns and seismic behavior of cold-formed thin-walled double C steel frame with gusset plate connected, this study has proved that such a cross-section framework has better seismic behavior. Further, the following conclusions have been drawn:

1. The final failure patterns of the three frames are similar. The framework's overall bending buckling after the web and flange were subjected to local buckling, both sides of pressured parts of the C steel stretched out and cracked, which would bring the bearing capacity of the C steel into full play. The degradation of the bearing capacity of this kind of structure is stable, and the energy dissipation capacity and ductility are superior to steel reinforced concrete and portal frame structures, an advantage of practical engineering applications.
2. Decreasing the pitch of bolts of beam-column joints could improve the bearing capacity and initial rigidity, but it would also reduce the energy consumption capacity and ductility, and accelerate rigidity degradation of the framework.
3. Decreasing the axial pressure ratio could improve the bearing capacity, ductility and energy dissipation capacity of the framework while reducing initial rigidity and accelerating rigidity degradation.

**ACKNOWLEDGEMENTS**

This study was carried out with the financial support of the National Science Foundation of China (Grant No.51368043)

**REFERENCES**

1. DeWolf John T., Pekoz Teoman and Winter T. George (1974). "Local and Overall Buckling of Cold-formed Steel Members", *J. Struct. Div., ASCE*, Vol. 100, No. 10, pp. 2017-2036.
2. Huang Zhi-guang (2010). "Seismic Behaviors Study on Low-rise Cold-formed Thin-walled Steel Residential Buildings", Doctoral Dissertation of Xi'an University of Architecture & Technology, Xi'an, ShanXi, China.
3. Huang Zhi-guang, Su Ming-zhou and He Bao-kang (2011). "The Three Layer Building Vibration Table Test of Cold-formed Steel", *China Civil Engineering Journal*, Vol. 44, No. 2, pp. 72-81.
4. Liu Fei, Li Yuan-qi and Shen Zu-yan (2009a). "Overview of Seismic Performance of Low-rise Cold-formed Thin-walled Steel Structure", *The 9<sup>th</sup> National Symposium on Modern Structural Engineering*, Ji'nan, China, pp. 142-149.
5. Liu Fei, Li Yuan-qi and Zhang Ji-cheng (2009b). "Analysis of Seismic Performance of Low-rise Cold-formed Thin-walled Steel Structure", *Journal of Yangtze University (Natural Science Edition), Sci & Eng*, Vol. 6, No. 1, pp. 91-95.
6. Schafer B.W. (2002). "Local, Distortional, and Euler Buckling of Thin-Walled Columns", *Journal of Structural Engineering, ASCE*, Vol. 128, No. 3, pp. 289-299.
7. Shen Zu-yan, Liu Fei and Li Yuan-qi (2013). "Seismic Design Method of Low-rise High-bearing Capacity Cold-formed Thin-walled Steel Framing Buildings", *Journal of Building Structures*, Vol. 34, No. 1, pp. 44-51.
8. Shi Yu, Zhou Xu-hong, Nie Shao-feng and Yuan Xiao-li (2011). "Seismic Dynamic Response Analysis for Cold-formed Steel Framing System of Mid-rise Residential Building", *Earthquake Resistant Engineering and Retrofitting*, Vol. 33, No. 5, pp. 7-12.
9. Wang Chun-han (2006). "Applying the Method in the Software of ANSYS High-bearing Capacity Bolt Pre-tightening Force", *Journal of Sichuan Building*, Vol. 26, No. 2, pp. 140-141.
10. Zhang Hong-bing and Du Jian-hong (1999). "Study on the Method of Applying Load of Bolt in the Finite Element Model", *Machinery Design & Manufacture*, No. 10, pp. 32-33.
11. Zhou Xu-hong, Shi Yu, Wang Rui-cheng and Li Ying (2008). "Cold-formed Steel Residential System for Rapid Reconstruction of the Earthquake-stricken Areas", *Wenchuan Earthquake Building Damages Analysis Report of the Investigation and Reconstruction*, China Architecture and Building Press, Beijing, China, pp. 442-447.